Full Length Article

Adsorption and self-assembling of a norbornadiene derivative on Au(1 1 1)

Suchetana Sarkar [a], Natasha Khera [a], Pedro Ferreira [b], Kwan Ho Au-Yeung [a,1], Pranjit Das [a], Roberto Robles [c], Nicolas Lorente [c,d], Kasper Moth-Poulsen [b,e,f], Francesca Moresco [a,*]

[a] Center for Advancing Electronics Dresden, TU Dresden 01062 Dresden, Germany
[b] Universitat Politècnica de Catalunya (UPC) & Institute of Materials Science of Barcelona (ICMAB-CSIC), Spain
[c] Centro de Física de Materiales CFM/MPC (CSIC-UPV/EHU), 20018 Donostia-San Sebastián, Spain
[d] Donostia International Physics Center, 20018 Donostia-San Sebastián, Spain
[e] Catalan Institution for Research & Advanced Studies, ICREAPg. Lluís Companys 23, 08010 Barcelona, Spain
[f] Department of Chemistry and Chemical Engineering, Chalmers University of Technology, SE-41296 Gothenburg, Sweden

ARTICLE INFO

ABSTRACT

The norbornadiene-quadricyclane photoswitch is a promising example of molecular solar thermal systems capable of energy conversion, storage and release. We present a scanning tunneling microscopy and spectroscopy study of a symmetric **NBD-COOMe** derivative adsorbed on the Au(1 1 1) surface, supported by density functional theory simulations. We observe the formation of ordered self-assembled islands of **NBD-COOMe** on the gold surface, driven by intermolecular van der Waals interaction, which become disordered and gradually desorb upon increasing the surface temperature. After annealing at 200 °C, a few adsorbed molecules show a different appearance and electronic structure suggesting the formation of single metalorganic complexes of **NBD-COOMe** with gold adatoms.

1. Introduction

As renewable energy systems such as solar and wind are introduced rapidly, energy storage is becoming increasingly important due to the daily and seasonal variability of energy production and demand. Several energy storage solutions, including battery, mechanical, and thermochemical solutions, are currently being explored to overcome this issue [1]. Meanwhile, there are many possible applications for smart energy management at a small scale. In this context, the so-called molecular solar thermal systems (MOST) are attracting increasing attention in the research community. The MOST concept is based on photoswitchable molecules that combine three essential functions: energy conversion, storage, and release [2–5]. This concept was introduced already in 1909 suggesting that it is possible using the anthracene dimerization reaction for solar energy storage [6]. Since then, several systems have been developed in both liquid and solid states [7–9]. One of the most promising MOST systems is based on the norbornadiene (NBD) – quadricyclane (QC) valence isomer. NBD is a bicyclic compound that undergoes [2 + 2] cycloaddition between the alkene moieties of the NBD to the photoisomer (QC) [9]. This process can be induced by light

irradiation [10] or under sensitizer conditions [11,12]. Moreover, versatile ways have been developed to trigger the release of the storage energy in QC to NBD conversion through optical, catalytical, electrocatalytic or thermal activation [13,14]. Furthermore, recent reports indicate that electronic activation can be used for energy storage and release processes, opening new opportunities for electronic memory systems [13]. In 2020, the reversibility of the NBD/QC system in a single molecule break junction (SMBJ) was reported. It was demonstrated that the NBD to QC isomerization arises from a local heating effect. At the same time, the reverse reaction is mainly catalyzed by a single charge-transfer process [15].
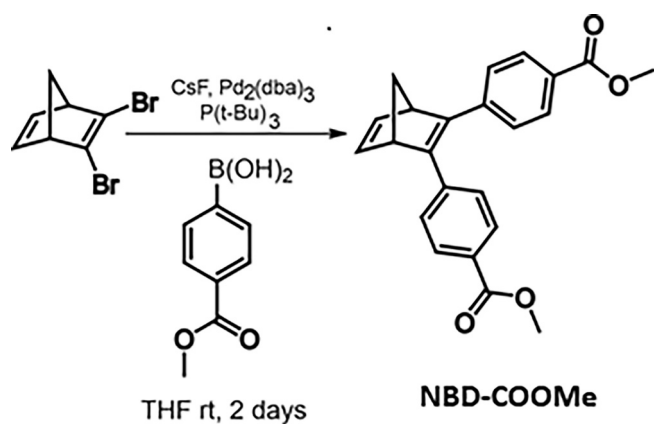
A further promising approach for energy storage in molecules is to exploit stable mechanical and electronic molecular excited states in molecular monolayers. This is possible by local conformational changes of the single molecules that can be induced by thermal or electrical excitation [16–18]. Advances in chemistry allow the synthesis of molecular switches whose conformational changes can be addressed in ensembles, setting the basis for realizing a new energy storage technology [19].

Studies have been performed on the interaction between the NBD

Scheme 1. Line drawing of the synthesis of **NBD-COOMe**.

and a surface, especially for studying the catalytic back reaction to extract the energy from the QC valence isomer [20–22]. In this context, the studies of a triazatriagulenium (TATA) and trioxatriagulenium (TOTA) platform decorated with an NBD on an Au(1 1 1) surface were reported [23], demonstrating the self-assembly of monolayers of TATA-NBD in long-range order, with no induced NBD to QC conversion tested either by a change in bias or light irradiation. Later, the same authors reported the catalytic effect of the gold surface in the back conversion of the QC to NBD in the TOTA-NBD derivative. The authors supported the latest by employing infrared reflection absorption spectroscopy (IRAS), demonstrating the QC to NBD isomerization of the TOTA derivative when it is in close contact with the surface [24].

Switching processes on single molecules adsorbed on a surface can be studied in detail under well-controlled ultra-high vacuum (UHV) conditions, allowing for fundamental model studies of potential molecule pairs and reaction that stores and releases energy. For applications in energy storage, it is also important to understand how molecules interact with the supporting metal surface, how stable they are at different temperatures, and how they break down or desorb.

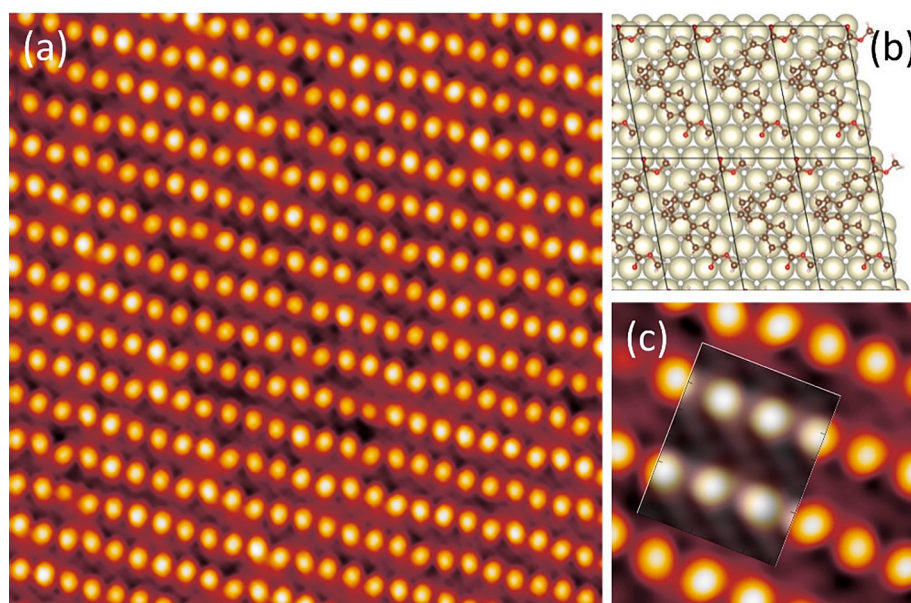Herein, we investigate an NBD derivative molecular system on the

Fig. 1. STM images and simulations of a self-assembled **NBD-COOMe** monolayer after deposition on Au(1 1 1). (a) Self-assembled monolayer showing an ordered structure of identical molecules. (b) DFT simulation of the adsorption geometry of **NBD-COOMe** in the monolayer. (c) Close-up of the island with the superposed simulated STM image corresponding to the geometry in (b). Image parameters: (a) V = 0.2 V, I = 100 pA, 20x20 nm^2 (b) V = 0.5 V, I = 30 pA, 5 × 5 nm^2. Simulated image in the inset.
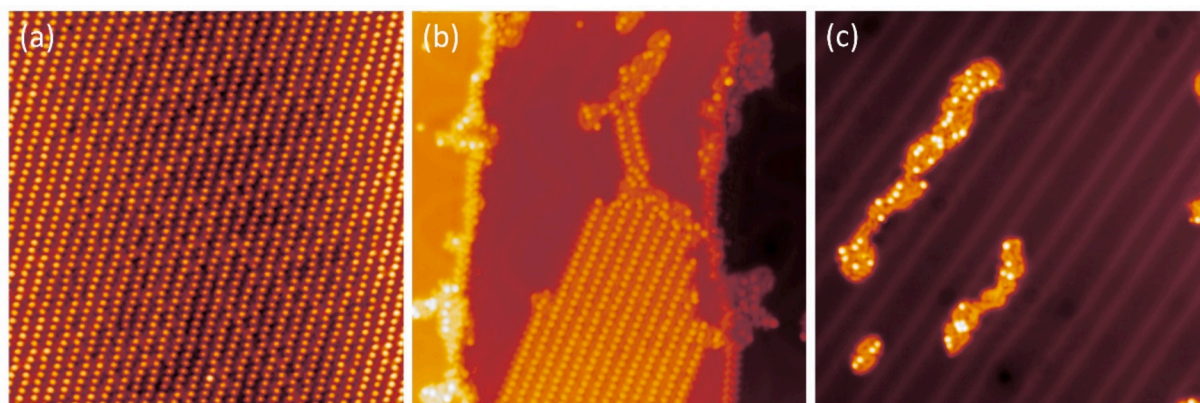

Fig. 2. Annealing steps. (a) Self-assembled monolayer after deposition at RT. (b) First annealing step at 200°C for 5 min. (c) Second step of annealing at 200 °C for 5 min. Image parameters: V = 0.2 V, I = 100 pA, 40 × 40 nm^2.
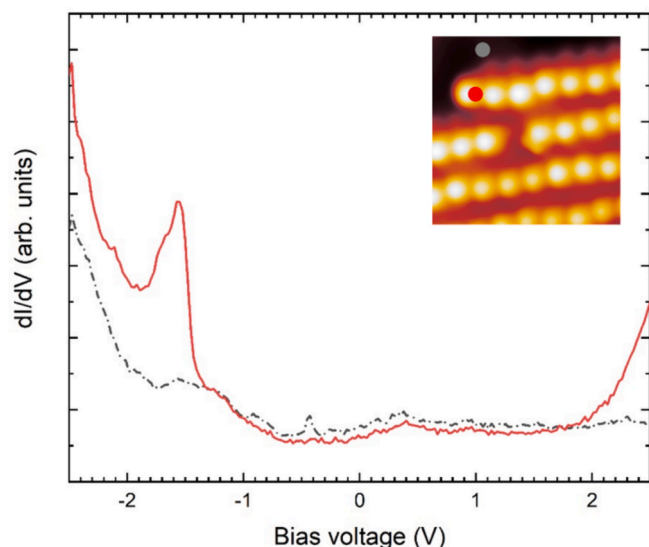
Fig. 3. Differential conductance spectrum of the molecule in the monolayer. Red curve: dI/dV spectrum recorded on the molecule indicated by a red dot in the inset. Dashed black curve: spectrum recorded on the Au(1 1 1) surface for comparison, at the position of the grey dot in the inset. Inset: STM image recorded at V = −2 V, I = 30 pA, size = 5 × 5 nm^2.

Au(1 1 1) surface using low-temperature UHV scanning tunnelling microscopy (STM) and spectroscopy (STS) supported by computational methods to understand the adsorption properties of these emerging energy storage systems. Furthermore, we aimed at exploring voltage induced structural changes induced by voltage pulses applied with the STM tip and the effect of thermal excitation. To this aim, we have synthesized a simple symmetrical norbornadiene derivative (**NBD-COOMe**), which incorporates ester derivatives (–COOMe) in terminal positions. The ester derivatives allow to maximize the interaction with the surface, while the symmetry of the molecule makes it easily identifiable by STM on the Au(1 1 1) surface. Upon adsorption on Au(1 1 1), we observe the formation of an ordered self-assembled monolayer driven by van der Waals interaction. By gradually increasing the surface temperature, the molecules partially desorb, while we observe a change in the appearance and electronic resonances of some molecules, which can be attributed to the formation of metalorganic complexes between NBD and gold adatoms.
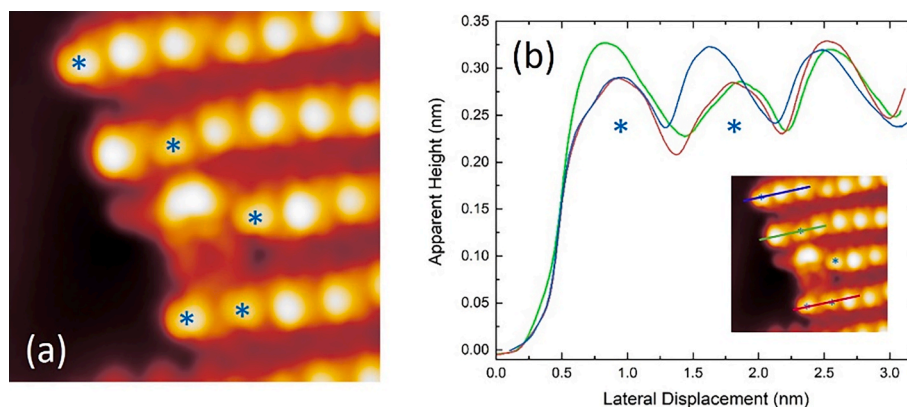
2. Methods

NBD-COOMe molecules were evaporated at 155 °C for 105 s onto a Au(1 1 1) surface kept at room temperature (25 °C). The Au (111) was then annealed to 200 °C, step-wise twice. For the hot deposition experiment, the molecules were evaporated at 170 °C for 90 s onto an Au (111) sample held at 200°C. Before evaporation, the gold substrate was cleaned by multiple cycles of Ar + sputtering and annealing to 450 °C. STM experiments were performed using a custom-built instrument operating at a low temperature of T = 5 K under ultrahigh vacuum (P ≈ 1 × 10^{-10} mbar). All shown STM images were recorded in constant-current mode with the bias voltage applied to the sample.

For spectroscopy experiments, all measurements were conducted in constant height mode. Spectra were measured using lock-in detection with a modulation frequency of 833 Hz and a modulation amplitude of 40 mV. Only metallic tips, i.e., tips showing the Au(1 1 1) surface state were used for spectroscopy measurements on the molecules.

Density functional calculations were performed using the Vienna ab initio simulation package (VASP) [25]. Core electrons were treated using the PAW formalism [26], while valence electrons were described using a plane-wave basis set with an energy cutoff of 400 eV. The PBE flavor of the GGA exchange and correlation functional was used [27], and it was completed with the Tkatchenko-Scheffler approximation to treat the missing van der Waals interactions [28], In order to simulate Au(1 1 1) surfaces we used a four layer slab separated by a 22 Å vacuum region. For the isolated molecules we used a (26.2 × 30.2) Å rectangular unit cell, while for the simulation of the self-assembled island we employed a (8.7 × 15.4) Å unit cell with an angle of 100.9°. The atomic positions of the molecules and the first two Au layers were relaxed until all forces were smaller than 0.01 eV/Å. STM images and dI/dV spectra were simulated using the STMpw code [29] following the Tersoff-Hamann [30] approximation and the method of Bocquet et al.[31].

3. Results and discussion

The norbornadiene derivative (**NBD-COOMe**) was designed with two para-ester phenyl rings attached on the same side of the norbornadiene (Scheme 1). The idea behind this design was to have a symmetric molecule to help visualize it on the surface despite symmetry around the double-bond of NBD being of some significance, because of the 3D nature of the unit. Any substitution with different groups would add chirality to the NBD, which could make the analysis of the STM images challenging. The ester motifs were also incorporated to increase the interaction between the molecule and the gold surface, as ester groups are known to interact well with gold surfaces [21].

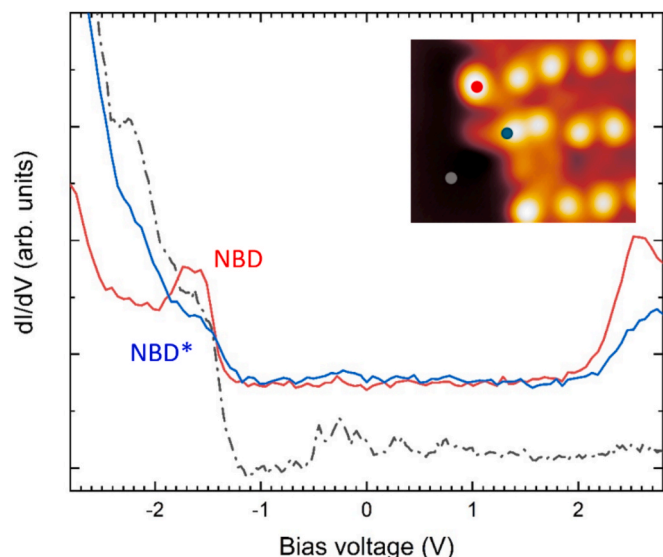**NBD-COOMe** was obtained, as shown in Scheme 1, via Suzuki cross-

Fig. 4. STM image after post-annealing at 200 °C recorded at a bias voltage of V = − 2 V. (a) Close-up of an island showing few NBD* (blue asterisk). Image parameters: V = −2 V, I = 50 pA, 6 × 6 nm^2 (b) Linescans over lines of molecules containing NBD*. The STM image in the inset shows the corresponding lines on the image with the same colors.

Fig. 5. STS on both conformers. Spectra taken on both NBD (**NBD-COOMe,** red) and NBD* (blue). NBD has an additional resonance below the Fermi energy compared to NBD*. Inset: V = 0.2 V, I = 100 pA, image size 5 nm × 4.5 nm. The colored dots indicate the position where the corresponding spectrum has been recorded.

coupling with the dibromo norbornadiene **1**, followed by column chromatography to yield the pure product in 33 %. The compound was characterised by high-resolution techniques, *e.g.* NMR spectroscopy and HRMS. Additional details can be found in the supporting information (SI) file.

The molecule was thermally evaporated in UHV conditions onto an Au(1 1 1) surface kept at room temperature. STM images are recorded after cooling the sample down to T = 5 K. We find that the surface is covered by an ordered close-packed molecular monolayer, as shown in Fig. 1. Each molecule appears as a well-rounded and distinct feature forming parallel lines. Domains with different orientations have also been observed (Fig. 2a and Fig. S8).

We determined the adsorption geometry of the **NBD-COOMe** monolayer on Au(1 1 1) via density functional theory (DFT) and image simulations, as shown in Fig. 1b and c. The simulated STM image of the self-assembled structure, visible in the inset of Fig. 1c, confirms that the pronounced central maximum is due to the NBD unit, appearing as a well-rounded central lobe at a small positive bias voltage. The side groups are oriented parallel to each other along the lines, while parallel lines of molecules form the two-dimensional monolayer structure, as shown in Fig. 1b. We also calculated the binding energy of single adsorbed molecules respect to the self-assembled monolayer. An

isolated molecule on the surface has a binding energy of 2.30 eV. For the molecule in the monolayer, it increases to 2.68 eV due to an increase of the van der Waals interaction of 0.44 eV. This demonstrates that the formation of the ordered monolayer is driven by the van der Waals interaction between the **NBD-COOMe** molecules.

To study the response of **NBD-COOMe** to thermal energy, we annealed the supporting surface during the molecule deposition or, similarly, post-annealed the substrate after deposition at RT. STM images were recorded at 5 K. After increasing the surface temperature to 150 °C and then 180 °C, respectively, we did not observe any change in the monolayer or of the molecular structure (see Fig. S9). On the other hand, post-annealing of the sample to 200 °C (Fig. 2) causes desorption and diffusion of molecules from the self-assembled structure (Fig. 2b). A further post-annealing at the same temperature (Fig. 2c) strongly reduces the molecular coverage on the surface. Fig. 2c also show the direction of the Au(1 1 1) surface reconstruction. The orientation of the domains in the self-assembled monolayer (Fig. 1, Fig. 2a, Fig. S8) is independent on the surface reconstruction, indicating a weak interaction between the molecule and the Au(1 1 1) surface. Deposition on the surface kept at T = 200 °C also shows a very low molecular coverage (see Fig. S10).

STS spectra recorded between V = −2.5 V and V = 2.5 V on the central NBD feature (Fig. 3) show a clearly visible electronic resonance at V = −1.6 V and an increasing background at higher positive voltage, in good agreement with DFT simulations for adsorbed **NBD-COOMe** showing two resonances corresponding to the highest occupied molecular orbital (HOMO) and lowest unoccupied molecular orbital (LUMO) of the molecule at V = −1.6 V and V = 2.2 V respectively. The slight bias-dependence observed in the STM images, where the NBD round feature is becoming more intense and diffuse at high negative bias already before annealing (see Figure S11), can be explained by an electronic contribution to the tunneling current related to the resonance at V = −1.6 V.

If we now image the surface after annealing at large negative voltage, we observe a different species of molecules (Fig. 4, Fig. S12) that we for the moment call NBD*. Fig. 4a shows a detail of an almost pristine island, where a few molecules (marked with blue asterisks) appear smaller and slightly elongated respect to **NBD-COOMe** when imaged at V = −2.0 V. To identify this new species of molecules we have compared in Fig. 4b linescans recorded along the self-assembled lines. We clearly see a difference in apparent height between the two species. It is important to note that the NBD* species appear in most cases close to the border of the island or in very small assemblies. This difference cannot be explained due to a change in orientation since the self-assembly is not disturbed.

We performed STS on the NBD* molecules and compared the spectra of the two species. Fig. 5 shows the differential conductance spectra of both **NBD-COOMe** and NBD* recorded in the same experimental
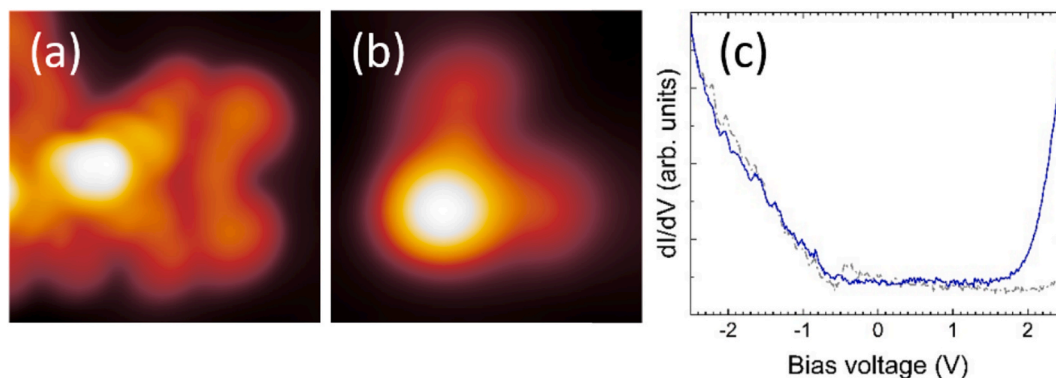

Fig. 6. STM images of single NBD* molecules (a) after annealing at 200 °C and stabilized by defects; (b) after deposition on the surface kept at T = 200 °C); (c) STS spectrum of the molecule in (b) confirming the quenching of the peak at −1.6 V. For both STM images: V = −2.0 V, I = 50 pA, image size 2.5x2.5 nm².
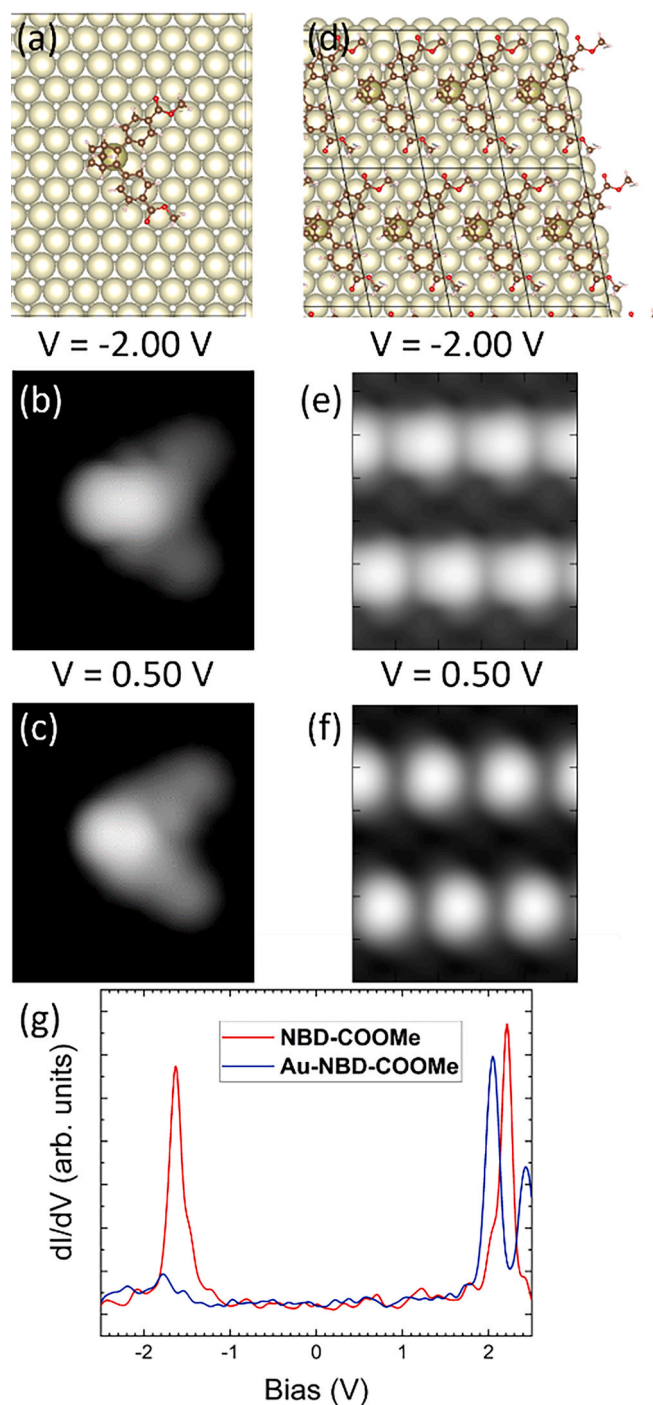
Fig. 7. DFT calculations of **Au-NBD-COOMe** complexes. (a) Top view of adsorption geometry of a single **Au-NBD-COOMe** complex on Au (1 1 1). (b) Calculated high bias STM topography of (a). (c) Calculated low bias STM topography of (a). (d) Top view of adsorption geometry of **Au-NBD-COOMe** complexes in a self-assembled island on Au (1 1 1). (e) Calculated high bias STM topography of (e). (f) Calculated low bias STM topography of (e). (g) Calculated dI/dV spectra of both species.

conditions. It is immediately apparent that **NBD-COOMe** (red curve) shows the resonance at −1.6 V below Fermi energy that we already presented in Fig. 3. This resonance is conspicuously absent in NBD* (blue curve). Similar dI/dV spectra taken on different molecules (see Fig. S13 and S14) show the same result, confirming that the negative resonance at around −1.6 V is quenched for NBD*.

In a few rare cases, after annealing at 200 °C or deposition on the hot surface, we could observe an isolated single molecule, either stabilized by defects (Fig. 6a) or as a single isolated molecule (Fig. 6b). The STS spectrum recorded on the isolated molecule (Fig. 6c) shows the same quenching of the resonance at −1.6 V, indicating that the isolated molecules are NBD*.

We performed DFT calculations to understand the nature of the NBD* species. The combination of STM, STS and DFT simulations is a reliable method to identify reactions and products also for rare on-surface synthesis reactions [32–34]. Since NBD is a well-known molecular switch, we considered first the possibility that NBD* is in reality the QC conformer. The reaction typically occurs in the gas phase through photoreaction [35] and, as mentioned earlier, was also observed through local heating in a single molecule tunnel junction [36]. However, it is known that the Au(1 1 1) surface presents a very high catalytic activity for the back-conversion from QC to NBD, thus making the QC isomer unstable on this surface [22,37]. Furthermore, the simulated STM images of **QC–COOMe** do not match our experimental results, especially at high voltages (see Fig. S15). Therefore, we can exclude a thermally-induced switching reaction of **NBD–COOMe** to **QC-COOMe** on the Au(1 1 1) surface. Also, the application of voltage pulses with the STM tip does not change the appearance of the molecules in the islands or on single isolated molecules.

Differently from the case of other MOST systems like azobenzene [18], we therefore exclude that the switching to the QC form can be thermally or electronically induced on this surface.

Dissociation reactions related to the catalytic ability of gold towards ester groups can also be excluded, and in the present investigation there is no evidence of oxygenate species forming strong bonds with gold. Previous studies have shown that aminolysis and esterification reactions are catalysed by gold, when esters and amines are present in suitable conditions [38]. However, these reactions seem to require a solvent or other reactants, which is not the case in the present work, performed in UHV conditions, *i.e.* completely free from any solvent. Additionally, the back-reaction of a different NBD decorated with ester groups was performed on Au(1 1 1) in a liquid phase. Even after 100 charge–discharge cycles, there was no indication of by-products or degradation [37].

However, we know from the literature that it is possible for the NBD to capture a gold adatom since it is an effective metal–ligand for norbornadiene-based complexes [39]. Metal surface adatoms are known to form complexes with single molecules in many different cases, contributing to stabilize structures and facilitating on-surface reactions [40–42]. Indeed, our DFT calculations suggest that NBD* is a complex between a **NBD-COOMe** molecule and a gold adatom. Fig. 7 show the adsorption geometry and simulated STM images at two different voltages for a single **Au–NBD–COOMe** complex (Fig. 7a-c) and for self-assembled molecular islands (Fig. 7d-f). The simulated images are in good agreement with the experimental STM images of NBD* presented in Figs. 4-6. In addition, the calculated dI/dV spectra shows a resonant state at −1.6 V for **NBD-COOMe**, and its suppression for the **Au–NBD–COOMe** complex, in agreement with the experiment in Fig. 5.

The origin of the adatom is readily explained by the thermal diffusion of gold adatoms from the step edges, favoured by the energy given to the surface during annealing. This would also account for the relatively low number of NBD* species and their location close to the edge of the islands.

4. Conclusions

In conclusion, we have presented a scanning tunneling microscopy and spectroscopy investigation of **NBD-COOMe** adsorbed on the Au(1 1 1) surface. We observe the formation of ordered self-assembled molecular islands, where the central core of the molecule appears as a round well-distinct feature. After annealing the surface at 200 °C most molecules desorb. At the same time, some of the remaining molecules are transformed in a metalorganic complex with a gold adatom, as confirmed by density functional theory calculations and image

simulations. Our results support the catalytic activity of Au(1 1 1), since no QC isomer could be observed. A new design decoupling the switching unit from the gold surface is needed to investigate NBD-QC systems triggered by tunneling electrons.

CRediT authorship contribution statement

Suchetana Sarkar: Writing – review & editing, Writing – original draft, Investigation, Formal analysis. **Natasha Khera:** Writing – review & editing, Investigation. **Pedro Ferreira:** Writing – review & editing, Investigation. **Kwan Ho Au-Yeung:** Writing – review & editing, Investigation. **Pranjit Das:** Investigation. **Roberto Robles:** Writing – review & editing, Investigation. **Nicolas Lorente:** Writing – review & editing, Investigation. **Kaspar Moth Poulsen:** Writing – review & editing, Investigation, Conceptualization. **Francesca Moresco:** Writing – review & editing, Writing – original draft, Investigation, Funding acquisition, Conceptualization.

Declaration of competing interest

The authors declare that they have no known competing financial interests or personal relationships that could have appeared to influence the work reported in this paper.

Acknowledgements

Appendix A. Supplementary data

Supplementary data to this article can be found online at https://doi.org/10.25532/OPARA-570.

Data availability

Supplementary data to this article can be found online at https://doi.org/10.25532/OPARA-570.

References

[1] O.S. Miljanic, J.A. Pratt, Introduction to Energy and Sustainability, Wiley, 2021.
[2] Z. Wang, P. Erhart, T. Li, Z.-Y. Zhang, D. Sampedro, Z. Hu, H.A. Wegner, O. Brummel, J. Libuda, M.B. Nielsen, K. Moth-Poulsen, Joule 5 (2021) 3116–3136, https://doi.org/10.1016/j.joule.2021.11.001.
[3] K. Moth-Poulsen, D. Ćoso, K. Börjesson, N. Vinokurov, S.K. Meier, A. Majumdar, P.C. Vollhardt, R.A. Segalman, Energy Environ. Sci. 5 (2012) 8534–8537, https://doi.org/10.1039/C2EE22426G.
[4] Z. Wang, H. Hölzel, K. Moth-Poulsen, Chem. Soc. Rev. 51 (2022) 7313–7326, https://doi.org/10.1039/D1CS00890K.
[5] K. Wang, H. Yu, J. Gao, Y. Feng, W. Feng, J. Mater. Chem. C 12 (2024) 3811–3837, https://doi.org/10.1039/d4tc00450g.
[6] F. Weigert, Ber. Dtsch. Chem. Ges. 42 (1909) 850–862, https://doi.org/10.1002/cber.190904201136.
[7] B. Tassignon, Z. Wang, A. Galanti, J. De Winter, P. Samorì, J. Cornil, K. Moth-Poulsen, P. Gerbaux, Chem. Eur. J. 29 (2023) e202303168, https://doi.org/10.1002/chem.202303168.
[8] B. Zhang, Y. Feng, W. Feng, Nanomicro Lett. 14 (2022) 138, https://doi.org/10.1007/s40820-022-00876-8.
[9] M. Jevric, A.U. Petersen, M. Mansø, S. Kumar Singh, Z. Wang, A. Dreos, C. Sumby, M.B. Nielsen, K. Börjesson, P. Erhart, K. Moth-Poulsen, Chem. Eur. J. 24 (2018) 12767–12772, https://doi.org/10.1002/chem.201802932.
[10] W.G. Dauben, R.L. Cargill, Tetrahedron 15 (1961) 197–201, https://doi.org/10.1016/0040-4020(61)80026-4.
[11] Y. Harel, A.W. Adamson, C. Kutal, P.A. Grutsch, K. Yasufuku, J. Phys. Chem. 91 (1987) 901–904, https://doi.org/10.1021/j100288a027.
[12] F.-Y. Meng, I.H. Chen, J.-Y. Shen, K.-H. Chang, T.-C. Chou, Y.-A. Chen, Y.-T. Chen, C.-L. Chen, P.-T. Chou, Nat. Commun. 13 (2022) 797, https://doi.org/10.1038/s41467-022-28489-0.
[13] B.E. Tebikachew, H.B. Li, A. Pirrotta, K. Börjesson, G.C. Solomon, J. Hihath, K. Moth-Poulsen, J. Phys. Chem. C 121 (2017) 7094–7100, https://doi.org/10.1021/acs.jpcc.7b00319.
[14] Z. Wang, A. Roffey, R. Losantos, A. Lennartson, M. Jevric, A.U. Petersen, M. Quant, A. Dreos, X. Wen, D. Sampedro, K. Börjesson, K. Moth-Poulsen, Energy Environ. Sci. 12 (2019) 187–193, https://doi.org/10.1039/C8EE01011K.
[15] H.B. Li, B.E. Tebikachew, C. Wiberg, K. Moth-Poulsen, J. Hihath, Angew. Chem. Int. Ed. 59 (2020) 11641–11646, https://doi.org/10.1002/anie.202002300.
[16] Z.J. Donhauser, B.A. Mantooth, K.F. Kelly, L.A. Bumm, J.D. Monnell, J.J. Stapleton, D.W. Price, A.M. Rawlett, D.L. Allara, J.M. Tour, P.S. Weiss, Science 292 (2001) 2303–2307, https://doi.org/10.1126/science.1060294.
[17] F. Moresco, G. Meyer, K.-H. Rieder, H. Tang, A. Gourdon, C. Joachim, Phys. Rev. Lett. 86 (2001) 672–675, https://doi.org/10.1103/PhysRevLett.86.672.
[18] M. Alemani, M.V. Peters, S. Hecht, K.-H. Rieder, F. Moresco, L. Grill, J. Am. Chem. Soc. 128 (2006) 14446–14447, https://doi.org/10.1021/ja065449s.
[19] Z.-Y. Zhang, Y. He, Z. Wang, J. Xu, M. Xie, P. Tao, D. Ji, K. Moth-Poulsen, T. Li, J. Am. Chem. Soc. 142 (2020) 12256–12264, https://doi.org/10.1021/jacs.0c03748.
[20] F. Hemauer, V. Schwaab, E.M. Freiberger, N.J. Waleska, A. Leng, C. Weiß, J. Steinhauer, F. Düll, P. Bachmann, A. Hirsch, H.-P. Steinrück, C. Papp, Chem. Eur. J. 29 (2023) e202203759, https://doi.org/10.1002/chem.202203759.
[21] F. Hemauer, H.-P. Steinrück, C. Papp, ChemPhysChem 25 (2024) e202300806, https://doi.org/10.1002/cphc.202300806.
[22] E. Franz, C. Stumm, F. Waidhas, M. Bertram, M. Jevric, J. Orrego-Hernández, H. Hölzel, K. Moth-Poulsen, O. Brummel, J. Libuda, ACS Catal. 12 (2022) 13418–13425, https://doi.org/10.1021/acscatal.2c03043.
[23] R. Löw, T. Rusch, T. Moje, F. Röhricht, O.M. Magnussen, R. Herges, Beilstein J. Org. Chem. 15 (2019) 1815–1821, https://doi.org/10.3762/bjoc.15.175.
[24] R. Eschenbacher, T. Xu, E. Franz, R. Low, T. Moje, L. Fromm, A. Gorling, O. Brummel, R. Herges, J. Libuda, Nano Energy 95 (2022), https://doi.org/10.1016/j.nanoen.2022.107007.
[25] G. Kresse, J. Furthmüller, Comput. Mater. Sci. 6 (1996) 15–50, https://doi.org/10.1016/0927-0256(96)00008-0.
[26] G. Kresse, D. Joubert, Phys. Rev. B 59 (1999) 1758–1775, https://doi.org/10.1103/PhysRevB.59.1758.
[27] J.P. Perdew, K. Burke, M. Ernzerhof, Phys. Rev. Lett. 77 (1996) 3865–3868, https://doi.org/10.1103/PhysRevLett.77.3865.
[28] A. Tkatchenko, M. Scheffler, Phys. Rev. Lett. 102 (2009) 073005, https://doi.org/10.1103/PhysRevLett.102.073005.
[29] N. Lorente, R. Robles, STMpw(v1.0b2), Zenodo (2019), doi: 10.5281/zenodo.3581159.
[30] J. Tersoff, D.R. Hamann, Phys. Rev. B 31 (1985) 805–813, https://doi.org/10.1103/PhysRevB.31.805.
[31] M.-L. Bocquet, H. Lesnard, S. Monturet, N. Lorente, Computational Methods in Catalysis and Materials Science (2009) 199–219, https://doi.org/10.1002/9783527625482.ch11.
[32] F. Eisenhut, T. Lehmann, A. Viertel, D. Skidin, J. Krüger, S. Nikipar, D.A. Ryndyk, C. Joachim, S. Hecht, F. Moresco, G. Cuniberti, ACS Nano 11 (2017) 12419–12425, https://doi.org/10.1021/acsnano.7b06459.
[33] D. Skidin, F. Eisenhut, M. Richter, S. Nikipar, J. Krüger, D.A. Ryndyk, R. Berger, G. Cuniberti, X. Feng, F. Moresco, Chem. Commun. 55 (2019) 4731–4734, https://doi.org/10.1039/C9CC00276F.
[34] K.H. Au-Yeung, T. Kühne, O. Aiboudi, S. Sarkar, O. Guskova, D.A. Ryndyk, T. Heine, F. Lissel, F. Moresco, Nanoscale Adv. 4 (2022) 4351–4357, https://doi.org/10.1039/D2NA00038E.
[35] A. Gimenez-Gomez, B. Rollins, A. Steele, H. Hölzel, N. Baggi, K. Moth-Poulsen, I. Funes-Ardoiz, D. Sampedro, Chem. Eur. J. 30 (2024) e202303230, https://doi.org/10.1002/chem.202303230.
[36] H.B. Li, B.E. Tebikachew, C. Wiberg, K. Moth-Poulsen, J. Hihath, Angew. Chem. Int. Ed. (2020).
[37] R. Eschenbacher, F. Hemauer, E. Franz, A. Leng, V. Schwaab, N.J. Waleska-Wellnhofer, E.M. Freiberger, L. Fromm, T. Xu, A. Görling, A. Hirsch, H.-P. Steinrück, C. Papp, O. Brummel, J. Libuda, ChemPhotoChem 8 (2024) e202300155, https://doi.org/10.1002/cptc.202300155.
[38] Y.-S. Bao, M. Baiyin, M. Agula, M. Jia, B. Zhaorigetu, J. Org. Chem. 79 (2014) 6715–6719, https://doi.org/10.1021/jo500877m.
[39] I. Chambrier, L. Rocchigiani, D.L. Hughes, P.M.H. Budzelaar, M. Bochmann, Chem. Eur. J. 24 (2018) 11467–11474, https://doi.org/10.1002/chem.201802160.

[40] J. Björk, C. Sánchez-Sánchez, Q. Chen, C.A. Pignedoli, J. Rosen, P. Ruffieux, X. Feng, A. Narita, K. Müllen, R. Fasel, Angew. Chem. Int. Ed. 61 (2022) e202212354, https://doi.org/10.1002/anie.202212354.

[41] R. Robles, V. Zobač, K.H. Au Yeung, F. Moresco, C. Joachim, N. Lorente, Phys. Chem. Chem. Phys. 22 (2020) 15208–15213, https://doi.org/10.1039/D0CP01657H.

[42] T. Kühne, K.H. Au-Yeung, F. Eisenhut, O. Aiboudi, D.A. Ryndyk, G. Cuniberti, F. Lissel, F. Moresco, Nanoscale 12 (2020) 24471–24476, https://doi.org/10.1039/D0NR06809H.